Saudi Journal of Biological Sciences 29 (2022) 998–1005

Contents lists available at ScienceDirect

Saudi Journal of Biological Sciences

journal homepage: www.sciencedirect.com

Original article

Cerebroprotective effect of Aloe Emodin: *In silico* and *in vivo* studies

Praveen Kumar Pasala [a], Rizwaan Abbas Shaik [b], Mithun Rudrapal [c,*], Johra Khan [d,e], Mohammad A. Alaidarous [d,e], Shubham Jagdish Khairnar [f], Atul R. Bendale [g], Vaishali D. Naphade [h,i], Ranjan Kumar Sahoo [j], James H. Zothantluanga [k], Sanjay G. Walode [c]

[a] *Santhiram College of Pharmacy, Nandyal 518501, Andhra Pradesh, India*
[b] *Creative Educational Society's College of Pharmacy, Kurnool 518003, Andhra Pradesh, India*
[c] *Rasiklal M. Dhariwal Institute of Pharmaceutical Education & Research, Pune 411019, Maharashtra, India*
[d] *Department of Medical Laboratory Sciences, College of Applied Medical Sciences, Majmaah University, Al Majmaah 11952, Saudi Arabia*
[e] *Health and Basic Sciences Research Center, Majmaah University, Al Majmaah 11952, Saudi Arabia*
[f] *MET Institute of Pharmacy, Bhujbal Knowledge City, Nashik 422003, Maharashtra, India*
[g] *Sandip Institute of Pharmaceutical Sciences, Nashik 422213, Maharashtra, India*
[h] *Department of Pharmacy, Oriental University, Indore 453555, Madhya Pradesh, India*
[i] *School of Pharmaceutical Sciences, Sandip University, Nashik 422213, Maharashtra, India*
[j] *School of Pharmacy and Life Sciences, Centurion University of Technology and Management, Bhubaneswar 752050, Odisha, India*
[k] *Department of Pharmaceutical Sciences, Faculty of Science and Engineering, Dibrugarh University, Dibrugarh 786004, Assam, India*

ARTICLE INFO

Article history:
Received 19 August 2021
Revised 25 August 2021
Accepted 30 September 2021
Available online 8 October 2021

Keywords:
Aloe emodin
Cerebroprotective
Cerebrotoxic proteins
MO/RCA
Molecular docking
Antioxidants

ABSTRACT

This study involved cerebroprotective potential of aloe emodin (AE) by *in silico* molecular docking analysis against various cerebrotoxic proteins followed by *in vivo* activity on multiple occlusions and reperfusion of bilateral carotid arteries (MO/RCA) induced cerebral injury in experimental rats. Molecular docking studies were carried out to evaluate the binding affinity (or binding interaction) between AE and various proteins involved in apoptosis such as caspase-3 (CASP3) and Bcl-2-associated X protein (BAX), and proteins involved in inflammation such as interleukin-6 (IL-6), tumor necrosis factor α (TNF α), nitric oxide synthase (NOS), acid-sensing ion channel (ASIC) and glutamate receptor (GR) involved in cerebral stroke, and results were compared with that of standard drugs, minocycline, quercetin, and memantine. Cerebral ischemic reperfusion induced by MO/RCA was assessed for 10 mins reperfusion period as one cycle, and the experiment was conducted for up to 3 cycles in rats. After completion of 3 cycles, the rats were subjected to ethically acceptable animal euthanasia followed by isolation of the brains which were studied for the size of cerebral infarction, and biochemical parameters such as glutathione (GSH), malondialdehyde (MDA), catalase (CAT) were estimated from the brain homogenate. Further, histological studies were done to study neuronal contact. Results of molecular docking indicated that the AE exhibited interaction with active sites of cerebrotoxic proteins usually involved in protein functions or cerebrotoxicity. Biochemical results showed that in the untreated brain, MDA levels increased significantly, and decreased GSH and CAT levels were observed when compared to MO/RCA group, while treated rats showed a decrease in the levels of MDA and an increase in GSH and CAT levels as compared to MO/RCA rats. In comparison with sham rats and normal rats, histopathological analysis revealed neuronal damage in MO/RCA surgery rats which manifested as decreased intact neurons. However, treatment with AE 50 mg/kg b.wt. restored contact between neuronal cells. It can be concluded that AE showed cerebroprotective effect on RO/RCA with promising inhibition of cerebrotoxic proteins (apoptotic and

* Corresponding author.
E-mail addresses: praveenpharmaco@gmail.com (P.K. Pasala), rsmrpal@gmail.com (M. Rudrapal), j.khan@mu.edu.sa (J. Khan), m.alaidarous@mu.edu.sa (M.A. Alaidarous), sunnykhairnar62@gmail.com (S. Jagdish Khairnar), atulbendale123@gmail.com (A.R. Bendale), vaishalinaphade587@gmail.com (V.D. Naphade), ranjankumar.sahoo@cutm.ac.in (R. Kumar Sahoo), jameshztta@gmail.com (J.H. Zothantluanga), sanjuwalode@rediffmail.com (S.G. Walode).

Peer review under responsibility of King Saud University.

Production and hosting by Elsevier

https://doi.org/10.1016/j.sjbs.2021.09.077

neuroinflammatory) as evident from molecular docking studies. The cerebroprotective potential of AE could be due to its anti-inflammatory, antioxidant, and antiapoptotic principles.

1. Introduction

Ischemic stroke is a common cerebrovascular disorder, and it commonly renders patients disabled or dead (Agarwal et al., 2000; Claibome, 1985). It is among the commonest causes of disability, dementia, and death in the developed world. Among the different types of stroke, 87 % of them were found to be a cerebral ischemic stroke. Acute brain injury or brain dysfunction is a result of cerebral ischemia which occurred due to impaired blood flow towards the brain. Despite advances in recent years with effective therapeutic techniques such as intravenous thrombolysis, anti-inflammatory, and neuroprotective medications, the majority of ischemic stroke patients still have a poor prognosis with severe neurological disability due to rapid neuronal destruction (Barnham et al. 2004; Bederson et al. 1986). An important role is played by mitochondria to regulate oxidative stress at the cellular level. Oxidative stress is the primary cause of ischemia/reperfusion (I/R) damage, according to various studies. As a result, decreasing cerebral I/R damage requires limiting mitochondrial malfunction produced by oxidative stress (Peter et al. 2005).

Aloe-emodin (AE) is an anthraquinone derivative that is naturally derived and is also an active ingredient of various medicinal plants like *Rheum palmatum* L., *Cassia occidentalis*, *Aloe vera* L., and *Polygonum multiflorum* Thunb. It has potential pharmacological activities including anticancer (George, 1959), antioxidant (George, 1959), anti-inflammatory (Farbiszewski et al. 1996), cardioprotective (Ginsberg et al. 1999; Guo et al. 2017), antifungal (Kang et al. 2021), antiviral (Vadivel et al. 2018), antibacterial (Hitoshi et al. 2020), antiplasmodial (Yasuhisa, 1978), immunosuppressive (Kumar et al. 2017), neuroprotective (Lin and Wang, 2016), hepatoprotective effects (Li-Hua et al. 2005) and dementia (Wen et al. 2008). Thus, AE has the potential to either be used for prophylaxis or for the treatment of cancers, malaria, viral infections, inflammatory disorders, type 2 diabetes, Alzheimer's disease and so on. In our current investigation, the cerebroprotective potential of AE was predicted by *in silico* molecular docking studies against proteins involved in apoptosis such as CASP3 and BAX and proteins involved in inflammation such as TNF α, IL-6, NOS, ASIC and GR. The cerebroprotective activity of AE was evaluated *in vivo* against MO/RCA induced cerebral injury in rats.

2. Materials and methods

2.1. Drugs, chemicals and reagents

Aloe emodin (Bimal Life Sciences, India), 2,3,5-Triphenyl tetrazolium chloride (TTC) (Sisco Research Laboratories Pvt. ltd., India), Thiobarbituric acid (Loba Chem. Pvt. ltd., India), *n*-butanol, (Merck Life Science Pvt. ltd., India) were procured and used without further purification.

2.2. Molecular docking simulation studies

The protein databank (PDB) (http://www.rcsb.org/) was used to retrieve the crystal structures of proteins, viz., BAX (PDB ID: 5 W60), TNF α (PDB ID: 5UUI), CASP3 (PDB ID: 2DKO), IL-6 (PDB ID: 1ALU), NOS (PDB ID: 6CIC), ASIC (PDB ID: 3S3X) and GR (PDB ID: 5ZG2). Preparation of the proteins was carried out with the Biovia Discovery Studio Visualizer (DSV) 2017 (Prepare protein protocol) at a physiological pH of 7.4. After downloading the 3D structures of protein molecules from the PDB database, water molecules, heteroatoms, and inhibitors were removed from the structures and the force field was applied to the protein molecule using DSV. The PubChem database was used to retrieve the Structure Data Format (SDF) of AE, minocycline (PubChem Id: 54675783), quercetin (PubChem Id: 5280343), and memantine (PubChem Id: 4054) (www.pubchem.ncbi.nlm.nih.gov/). The DSV was used to prepare and protonate ligands at a physiological pH of 7.4, and minimization of their geometry was also carried out.

The proteins were energetically minimized and active sites were predicted with the selection of maximized GRID parameters using DSV. Protein-ligand docking studies were performed between AE and target proteins (as depicted above) with standard docking protocol using the AutoDock Vina of the PyRx virtual screening platform (Oleg and Olson, 2010). Docking results of AE were compared with that of standard molecules, minocycline, quercetin, and memantine (Stefan and Gudrun, 1974). The DSV 2017 R2 software was used to visualize the proteins and the protein–ligand complexes, and the PyRx tool was used for the calculation of binding energies (kcal/mol) for the docked complexes (Oleg and Olson, 2010). Higher negative binding energy indicates higher binding affinity. Higher docked scored complexes were evaluated for the analysis of binding interactions using DSV.

2.3. Cerebroprotective activity

The Institutional Animal Ethics Committee (IAEC/CESCOP/2019-OCT-06) approved the animal study protocol and animals were maintained as per CPCSEA guidelines. Wistar albino adult rats of either sex were categorized into groups of five wherein six rats were allocated to all the groups such as group I (normal control), group II (sham control), and group III (disease control). Group IV and Group V served as pre-treatment groups of AE for 10 days at a dose of 25 and 50 mg/kg b.wt. i.p., respectively which was followed by MO/RCA surgery. After 3 cycles were completed, the rats were subjected to ethically acceptable animal euthanasia followed by isolation of the brains for the measurement of cerebral infarction size. The estimation of GSH (Inan and Ozyurt, 2012), SOD (Dong-Ju et al. 2020; Hait et al. 2013), MDA (Hait et al. 2013), and CAT (Cristina et al. 2002) were carried out with the brain homogenate.

MO/RCA surgery was performed under anesthetized condition using Ketamine and xylazine (60 and 10 mg/kg b.wt., respectively). Separation of common carotid arteries from all muscles, ligaments, their adventitial sheath, and vagus nerves was carried out. They were then occluded for 10 mins followed by reperfusion for 10 mins. This entire process was considered as one cycle. The experiment was continued for up to 3 cycles. After 3 cycles were completed, parameters such as pupil dilation, locking of cornea reflex, limb reflexes, and temperature of rectal were observed (Emine et al. 2018). A heating lamp was used to prevent the development of hypothermia.

2.4. Histopathological study

A freshly prepared 10 % neutral buffered formalin was used to fix the sagittal brain sections and these were fixed in paraffin. For histopathological examinations, paraffin sections with a

Table 1
Binding energies and interaction details of AE-proteins complexes.

Ligand	Target protein	Binding energyPyRx (-kcal/mol)	Hydrogen bond	pi-pi bond	pi-alkyl bond	pi-sigma bond	pi-anion bond	Amide-pi bond	Alkyl bond
AE	BAX (Chain A)	6.5	ARG89 (2.50 Å)	PHE93 (3.56 Å)					
	TNF α (Chain A)	7.6	VAL150 (1.74 Å), ALA33 (1.90 Å)		ALA18 (3.38 Å), PRO20 (4.18 Å), VAL17 (4.05 Å), ARG32 (4.35 Å)				
	CASP3	6.7	HIS A:121 (1.85 Å), ARG B:207 (2.23 Å), GLN A:161 (2.62 Å)	PHE B:256 (4.22 Å)					
	IL-6(Chain A)	6.8	ASN63 (1.80 Å)	LEU147 (4.23 Å)		TYR97 (4.12 Å)			
	NOS (Chain A)	9.1	GLN162 (1.96 Å)	TRP414 (3.68 Å), PHE589 (4.10 Å)	CYS420 (1.55 Å)				
	ASIC	8.0	ARG B: 270 (1.63 Å), GLU A: 417 (1.75 Å), GLU B: 374 (1.85 Å), LYS C: 373 (2.22 Å), GLY B: 279 (2.65 Å), ARG C: 370 (2.69 Å)						
	GR(Chain A)	8.4	THR501 (1.56 Å), TYR753 (2.36 Å)	TYR471 (4.15 Å)	MET279 (4.35 Å)		GLU726 (3.16 Å), GLU423 (4.32 Å)		
Minocycline	BAX(Chain A)	6.2	ASP98 (1.90 Å) ASP102 (2.03 Å)		VAL180 (4.05 Å)			GLY179 (3.89 Å)	
	TNF α (Chain A)	7.1	ASP140 (1.93 Å), LYS65 (1.95 Å), PHE144 (2.19 Å), PRO20 (2.35 Å)						
	CASP3	7.4	HIS A: 121 (1.55 Å), ARG B: 207 (2.22 Å), CYS A: 163 (2.52 Å)						
	IL-6 (Chain B)	6.6	TRP592 (1.85 Å), GLU597 (2.85 Å)		VAL B: 572 3.98 Å), MET575 4.25 Å),				PHE589 (4.32 Å), CYS420 (4.52 Å)
	NOS (Chain A)	8.8	ARG104 (1.95 Å), GLN156 (2.55 Å), GLU106 (3.98 Å)			PHE105 (4.58 Å)			
Quercetin	ASIC	9.3	GLU C: 98 (1.62 Å), ARG C: 191 (1.85 Å), GLU C: 154 (2.32 Å), ARG F: 28 (2.62 Å), SER C: 241 (2.74 Å), GLU C: 243 (2.82 Å)						
Memantine	GR (Chain B)	5.6	GLN663 (2.25 Å), SER661 (2.56 Å)		TYR694 (3.62 Å, LYS690 (4.22 Å)				

thickness of 4 μm were prepared and hematoxylin and eosin (H&E) were used to stain these sections which were examined under 40 times magnification with a light microscope (Wen-yi et al. 2013).

2.5. Statistical analyses

Data were given as mean ± SEM for triplicate studies. A significant difference between groups was calculated by *t*-test and one-way analysis of variance (ANOVA) followed by the Dunnet comparison test. Mean values with $p < 0.05$ were considered statistically significant.

3. Results

3.1. Docking analysis

In the docking study, AE showed favorable binding affinities against BAX, TNF α, NOS, IL-6, and NOS as compared to the standard compound, minocycline, and against chain A of ASIC and GR compared to quercetin and memantine (Table 1).

For BAX, AE interacted with chain A of the protein. AE formed hydrogen bonds (H bonds) with ARG89 (bond distance = 2.50 Å) and pi-pi stacked with PHE93 (bond distance = 3.56 Å). AE has a binding affinity of −6.5 kcal/mol towards BAX. Minocycline formed H bonds with ASP98 and ASP102 (bond distances = 1.90 Å and 2.03 Å, respectively), amide-pi stacked with GLY179 (bond distance = 3.89 Å), and pi-alkyl bond with VAL180 (bond distance of 4.05 Å). Minocycline has a binding affinity of −6.2 kcal/mol towards BAX.

For TNF α, AE interacted with chain A of the protein. AE formed H bonds with VAL150 and ALA33 (bond distances = 1.74 Å and 1.90 Å, respectively), pi-alkyl with ALA18, PRO20, VAL17, ARG32 (bond distances = 3.38 Å, 4.18 Å, 4.05 Å, and 4.35 Å, respectively). AE has a binding affinity of −7.6 kcal/mol towards TNF α. Minocycline formed H bonds with ASP140, LYS65, PHE144, PRO20 (bond distances = 1.93 Å, 1.95 Å, 2.19 Å, and 2.35 Å, respectively). Minocycline has a binding affinity of −7.1 kcal/mol towards TNF α.

For CASP3, AE formed H bonds with HIS A:121, ARG B:207, and GLN A:161 (bond distances = 1.85 Å, 2.23 Å and, 2.62 Å, respectively), and pi-pi bond with PHE B:256 (bond distance = 4.22 Å). AE has a binding affinity of −6.7 kcal/mol towards CASP3. Minocycline formed H bonds with HIS121, ARG207, CYS163 (bond distances = 1.55 Å, 2.22 Å and, 2.52 Å, respectively). Minocycline has a binding affinity of −7.4 kcal/mol towards CASP3.

For IL-6, AE interacted with chain A of the protein. AE formed H bonds with ASN63 (bond distances = 1.80 Å), pi-sigma bond with TYR97 (bond distance of 4.12 Å), and pi-pi bond with LEU147 (bond distances = 4.23 Å). AE has a binding affinity of −6.8 kcal/mol

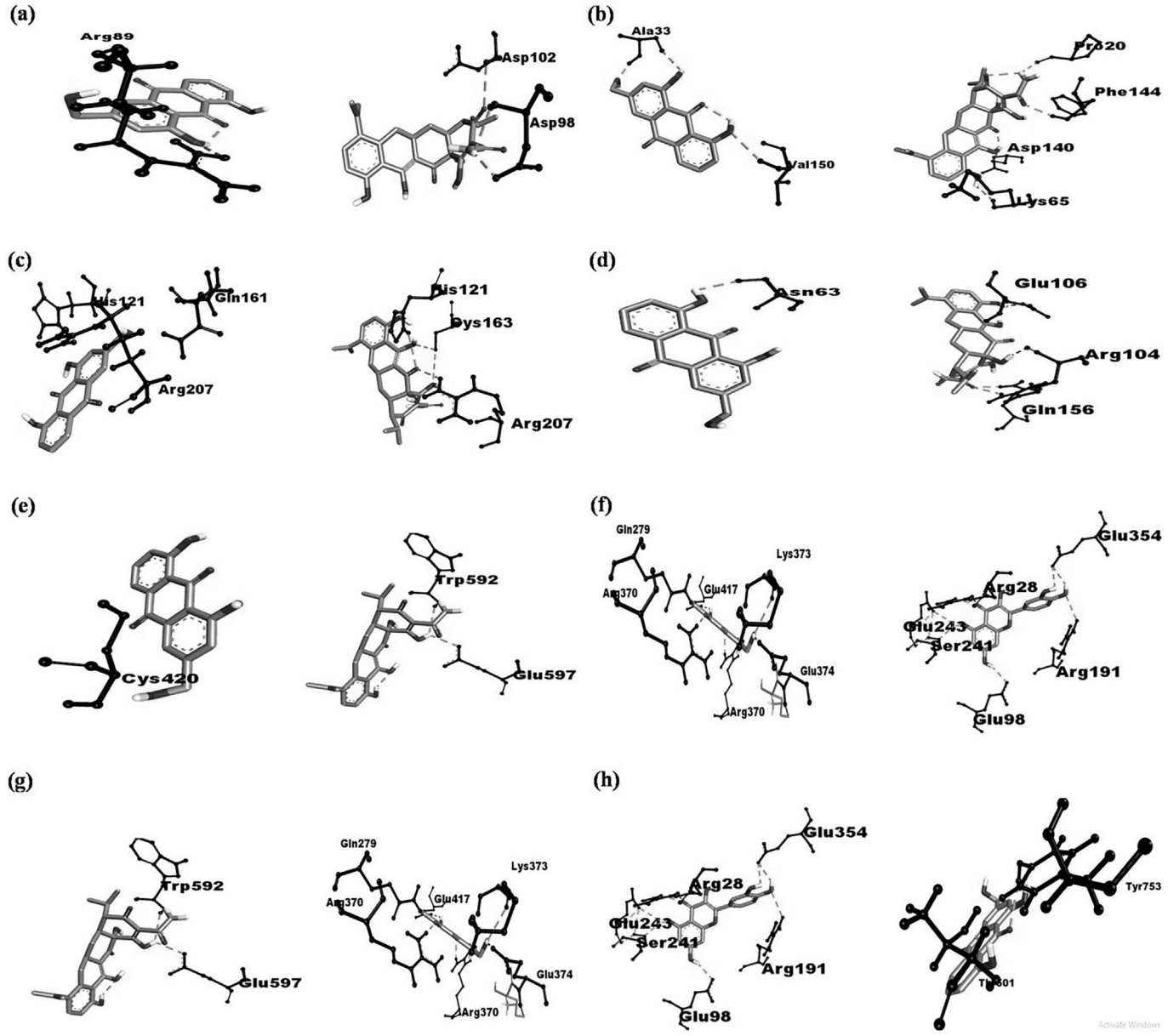

Fig. 1. 2D diagrams of AE-protein complexes: (**a**) AE-BAX (left), Minocycline-BAX (right); (**b**): AE-TNF α (left), Minocycline-TNF α (right); (**c**): AE-CASP (left), Minocycline-CASP (right); (**d**): AE-IL-6 (left), Minocycline-IL-6 (right); (**e**): AE-NOS (left), Minocycline-NOS (right); (**f**): AE-ASIC (left), Quercetin-ASIC (right); (**g**): AE-ASIC (left), Quercetin-ASIC (right); (**h**): AE-GR (left), Memantine-GR (right).

towards IL-6. Minocycline formed H bonds with ARG104, GLN156, and GLU106 (bond distance = 1.95 Å, 2.55 Å, and 3.98 Å, respectively), pi-sigma bond with PHE105 (bond distance = 4.58 Å). Minocycline has a binding affinity of −6.6 Kcal/mol towards IL-6.

Against NOS, AE interacted with chain B of the protein. AE formed H bonds with CYS420 (bond distance = 1.12 Å), pi-pi bond with PHE589 (bond distance = 4.02 Å). AE has a binding affinity of −9.1 kcal/mol towards NOS. Minocycline formed H bonds with TRP B:592, GLU B:597 (bond distances = 1.85 Å and 2.85 Å respectively), pi-alkyl bond with VAL B:572, MET B:575 (bond distances = 3.98 Å and 4.25 Å, respectively), and alkyl bond with PHE B:589 (bond distance of 4.32 Å). Minocycline has a binding affinity of −8.8 kcal/mol towards NOS.

Against ASIC, AE formed H bonds with ARG B:270; GLU A: 417; GLU B: 374, LYS C:373, GLY B:279, ARG C:370 (bond distance = 1. 63 Å, 1.75 Å, 1.85 Å, 2.22 Å, 2.65 Å, and 2.69 Å, respectively). AE has a binding affinity of −8.0 kcal/mol towards ASIC. Quercetin formed H bonds with GLU C:98, ARG C:191, GLU C:154, ARG F:28, SER C:241, GLU C:243 (bond distance of 1.62 Å, 1.85 Å, 2.32 Å, 2.62 Å, 2.74 Å and 2.82 Å, respectively). Quercetin has a binding affinity of −9.3 kcal/mol towards ASIC.

For GR, AE interacted with chain A of the protein. AE formed H bonds with TYR753 and THR501 (bond distances = 1.52 Å and 2.35 Å, respectively), pi-alkyl bond with TYR471, and MET279 (bond distances = 3.16 Å and 4.35 Å, respectively). AE has a binding affinity of −8.4 kcal/mol towards GR. Memantine formed H bonds with GLN B:663 and SER B:661 (bond distances = 2.25 Å and 2.56 Å, respectively), pi-alkyl bond with TYR B:694 and LYS B:690 (bond distances = 3.62 Å and 4.22 Å, respectively). Memantine has a binding affinity of −5.6 kcal/mol. Fig. 1 depicts detailed 2D interaction diagrams of AE-proteins complexes.

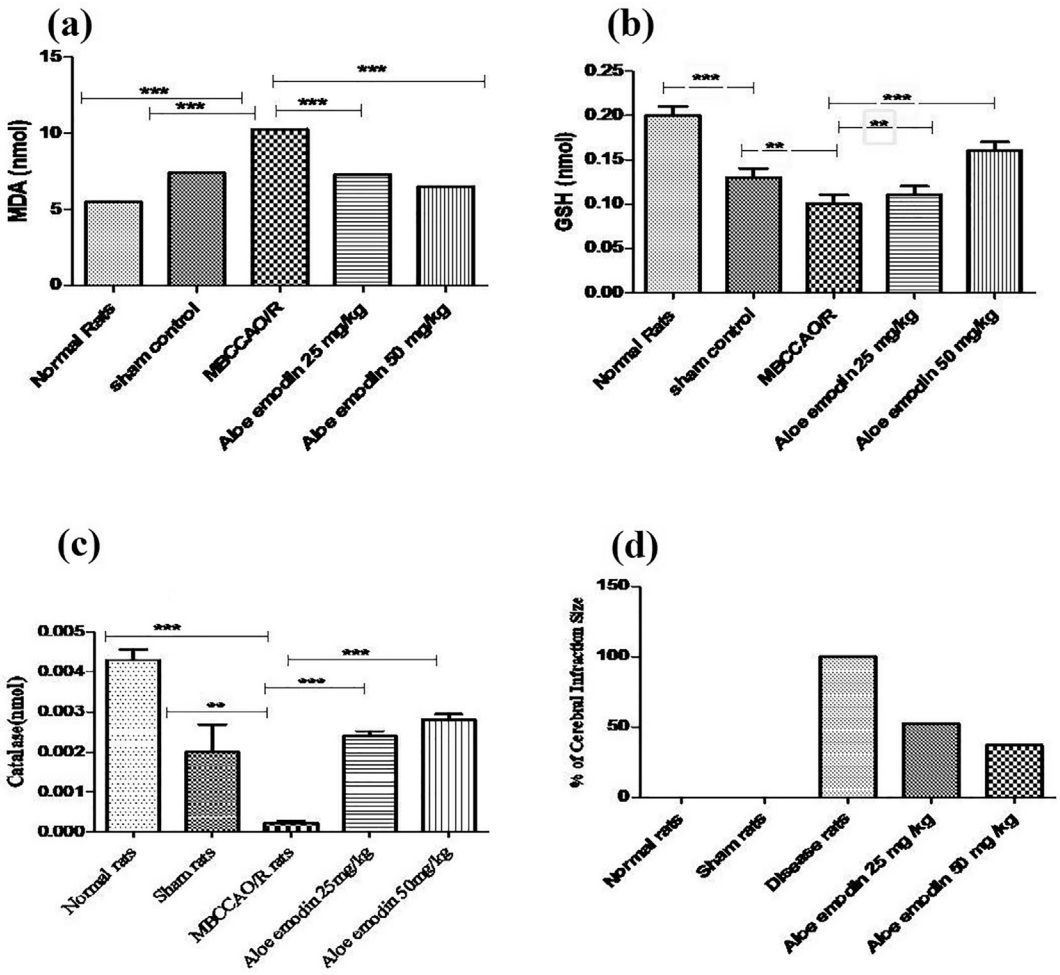

Fig. 2. Statistical representation of the impact of AE on brain biochemical parameters: (**a**) MDA, (**b**) GSH, (**c**) CAT, and (**d**) percentage of infarction size in the cerebrum of MO/RCA rats.

3.2. Cerebroprotective activity

In comparison to normal and sham rats, biochemical studies revealed that brain MDA levels increased significantly (10.28 ± 0.20 nmol/mg) in MO/RCA rats. In AE treated rats (25 and 50 mg/kg b.wt.), MDA levels decreased significantly ($p < 0.0001$) (7.27 ± 0.20 nmol/mg, 6.48 ± 0.009 nmol/mg) in comparison to sham rats, respectively. In comparison to normal and sham rats, brain GSH levels was significantly decreased (0.10 ± 0. 01 nmol/mg) in MO/RCA, while GSH levels significantly increased ($p < 0.1395$ and $p < 0.0004$) in AE treated rats (25 mg/kg b.wt., 0. 11 ± 0.01 nmol/mg and 50 mg/kg b.wt. 0.16 ± 0.01 nmol/mg). Brain CAT levels were significantly decreased (0.00022 ± 0.00005 nmol/mg) in MO/RCA rats, while CAT levels significantly increased ($p < 0.0001$, $p < 0.0001$, $p < 0.0026$) in AE treated rats (25 mg/kg b. wt., 0.0024 ± 0.00011 and 50 mg/kg b.wt., 0.0028 ± 0.00014). In comparison to the normal group and control group, the percent cerebral infract was significantly increased in MO/RCA group. Results are shown in Fig. 2 and Table 2.

In comparison to the MO/RCA group, cerebral infarction volume was significantly decreased to 47.75 % and 63.12 % in AE (25 and 50 mg/kg b.wt., respectively) which indicated that AE treatment exerts cerebroprotective activity (Fig. 3). In comparison to the rest of the groups, the histopathological study revealed that MO/RCA rats showed decreased neuronal cell intensity, increased form of the shrunken and irregular shape of a neuronal cell in the hippocampus region of the brain. Decreased intact of neurons and neuronal in MO/RCA group was reverted in AE treated rats (Fig. 4).

Table 2
Effect of AE on the biochemical parameters of the hippocampus of the brain in rats injured by MO/RCA surgery.

Treatment	Infarction size (%)	Concentration (nmol/mg)		
		GSH	MDA	CAT
Normal rats	0	0.2 ± 0.01***	5.4 9 ± 0.10***	0.0043 ± 0.00025***
Sham rats	0	0.13 ± 0.01**	7.41 ± 0.20***	0.0020 ± 0.00068**
MO/RCA	100 %	0.10 ± 0.01***	10.28 ± 0.20***	0.00022 ± 0.00005***
AE 25 mg/kg	47.75 %	0.11 ± 0.01**	7.27 ± 0.20***	0.0024 ± 0.00011***
AE 50 mg/kg	63.12 %	0.16 ± 0.01***	6.48 ± 0.09***	0.0028 ± 0.00014***

The data are expressed in the Mean ± Standard error of mean (SEM) of triplicate studies. Mean values of the difference between groups with $p < 0.05$*, $p < 0.01$**, $p < 0.001$*** are considered to be statistically significant.

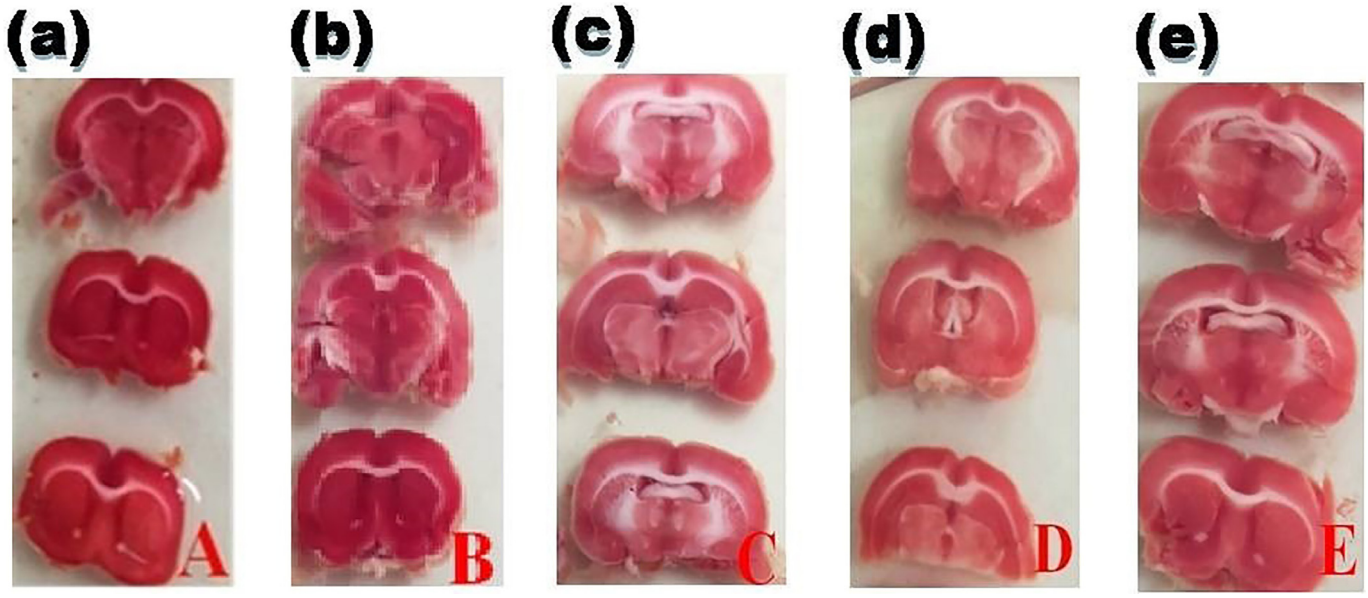

Fig. 3. AE inhibits MO/RCA with an increase in the percentage of the volume of cerebral infarction of rats: (**a**) Normal group, (**b**) Sham group, (**c**) MO/RCA group, (**d**) MO/RCA + 25 mg/kg b. wt. of AE treated group, (**e**) MO/RCA + 50 mg/kg b. wt. of AE treated group.

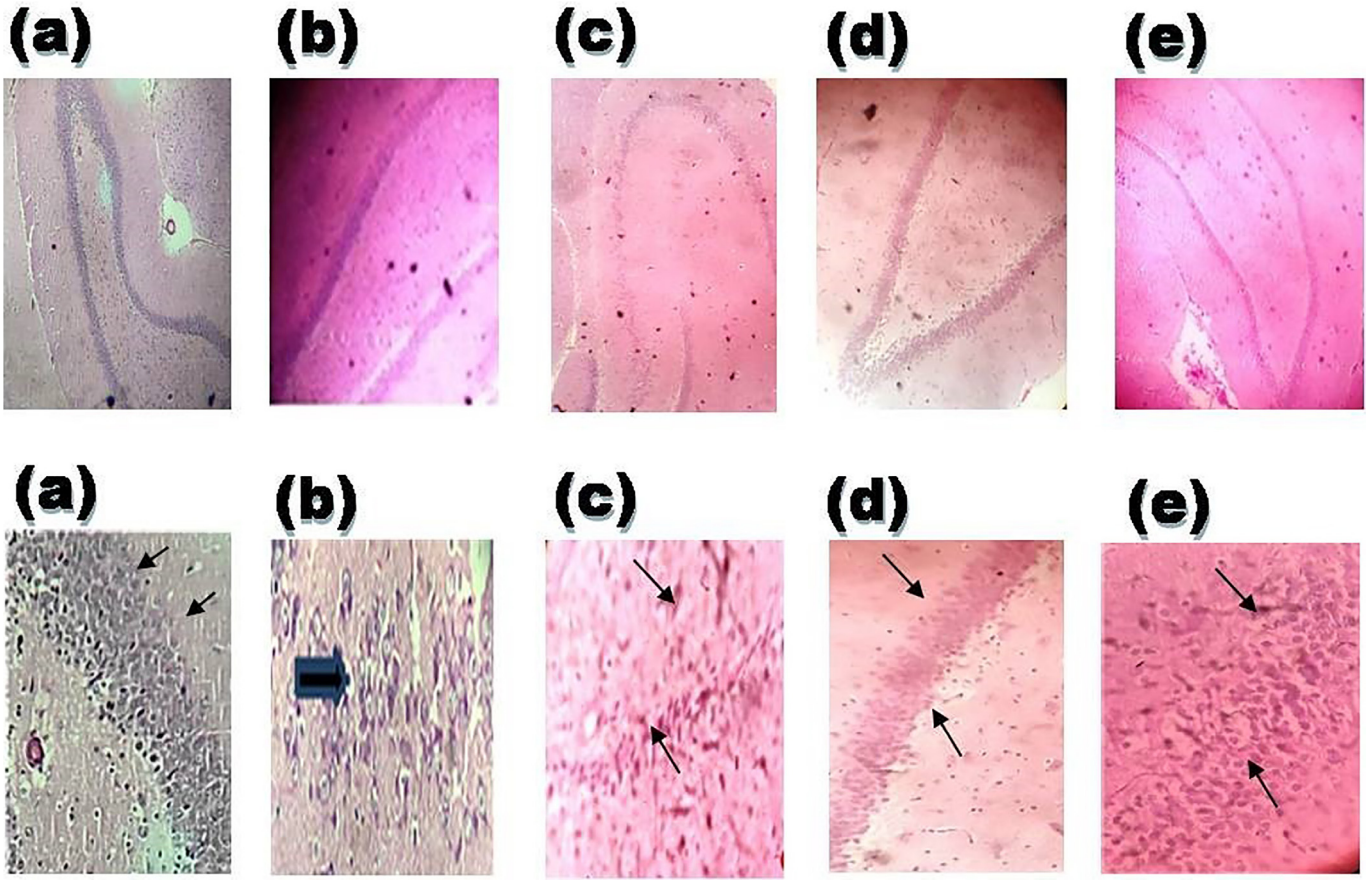

Fig. 4. Visualization of the hippocampus region of the brain of rats after MO/RCA surgery. 40 times magnification of the hippocampus region of the brain after cerebral stroke was induced: (**a**) Normal group, normal neuronal cell (black arrow), (**b**) Sham group; (**c**) MO/RCA group, (**d**) MO/RCA + 25 mg/kg b. wt. of AE treated group, (**e**) MO/RCA + 50 mg/kg b. wt. of AE treat group. The neuronal cells in the hippocampus region of the treated rats are less scattered (indicated by the black arrow). The thickness of the pyramidal cell layer was found to be increased in the treated rats while a decrease in apoptotic neurons with dystrophic changes was observed as shrunken and irregular (indicated by black arrows).

4. Discussion

Among the different types of stroke, high morbidity and mortality in humans are attributed to ischemic stroke. Ischemic stroke is marked by cerebral ischemia/reperfusion damage, which happens when blood flow is restored after a brief brain artery obstruction (Vesna et al. 2011). Stroke, ischemia, or inflammation can induce the release of glutamate or ATP that can further trigger different signaling cascades which can ultimately lead to neuronal injury and apoptotic cell death (Sharanya et al. 2020; Fengge et al. 2020; Marc et al. 2007; Tabassum et al. 2013; Li et al. 2014; Era and Probert, 2008; Wei et al. 2018). After cerebral ischemia/reperfusion, oxidative stress induced by increased production of ROS can result in the death of neurons, and several studies had reported the abnormality of oxidant enzymes, such as GSH, MDA, and CAT in ischemic stroke (Turley et al. 2005; Palo et al. 1988; Hwang et al. 1998). Neutralization of ROS ($O2^{\bullet -}$, $OH^{\bullet}$, H_2O_2, and lipoperoxides) occurs when GSH (an endogenous non-enzymatic antioxidant) reacts with ROS to be oxidized into GSSG (Song et al. 2020; Jingxian et al. 2013). The ratio of GSH/GSSG is regarded as a reliable indicator for the presence of ROS (Jingxian et al. 2013). The levels of GSH in MO/RCA rats were decreased in this study, whereas GSH levels were restored in AE-treated rats. Malondialdehyde (MDA) has long been employed as a marker of lipoperoxidation, which is primarily induced by hydroxyl free radical damage ($OH^{\bullet}$) (Xiong et al. 2008). After MO/RCA, an increase in the levels of MDA was observed. However, AE treatment reduced MDA levels significantly.

Our results advocate that AE offers protection against MO/RCA-induced oxidative stress by decreasing the levels of ROS and MDA while it increases GSH and CAT levels. Several studies have demonstrated that ischemia/reperfusion triggers a deleterious chain of events that include inflammation, apoptosis, production of ROS, and excitotoxicity which causes neuronal death including hippocampal neurons (Tiansong et al. 2020). Loss of neuronal cell contact resulted in morphological abnormalities in brain neurons in MO/RCA rats, according to histopathological studies. In MO/RCA rats, pre-treatment with AE enhanced neuronal cell contact, neuronal morphological modification, and neuronal diseases in the brain region, indicating that AE has a protective effect in the MO/RCA design.

The study also involved molecular docking studies of AE on proteins involved in apoptosis (BAX and CASP3), and proteins involved in inflammation (TNF α, IL-6, ASIC, and GR) to assess the binding affinity in terms of binding energy and interaction. These cerebrotoxic proteins are over-expressed during neuroinflammation (Wei et al. 2021; Yu et al. 2019), and ASIC leads to neuronal injury which is mediated by acidosis (Mavdzhuda et al. 2013). Results of docking showed that AE exhibited interactions with TNF α active sites of VAL A:17, 150, ALA A:17, 18, 33, PRO A:20, ARG A:32; CASP3 active sites of HIS A:121, ARG B:207, TRP A:414, CYC A:420; NOS active sites of PHE A:589, and GR (chain A) active sites of THR501, TYR753, GLU726, and TYR471. From molecular docking results, it can be concluded that AE interferes with the function of TNF α, CASP3, NOS, and GR through H Bonding and hydrophobic interactions, which might suppress the disease progression. Minocycline (standard compound) formed H bonding with CASP3 active sites of HIS A:121, CYS A:163, and ARG B:207; with TNF α (chain B) active sites of TRP592, GLU597, hydrophobic interactions on NOS (chain B) active sites of VAL572, MET575, PHE589, VAL421, and H bonding on IL-6 active sites of GLN A:156. Results revealed that AE exhibited a strong inhibitory effect on TNF α, CASP3, NOS, and GR, suggesting its strong protective effect against MO/RCA induced cerebral injury (cerebral ischemia/reperfusion damage) in rats. The cerebroprotective function of AE might be mediated through its antioxidant, anti-inflammatory, and antiapoptotic actions.

5. Conclusion

The findings of our present investigation suggest a potential protective role of AE against MO/RCA assault, which might be linked to the antioxidant capacity of AE. The inhibitory potential of AE against cerebrotoxic (apoptotic and neuroinflammatory) proteins was demonstrated by *in silico* docking analysis. Further *in vivo* studies are required at the molecular level (identifying the exact biological target / biochemical pathways) to explore the therapeutic potential of AE as a neuroprotective in cerebral ischemic stroke.

Declaration of Competing Interest

The authors declare that they have no known competing financial interests or personal relationships that could have appeared to influence the work reported in this paper.

Acknowledgement

The authors would like to thank the Deanship of Scientific Research at Majmaah University for supporting this work under Project number (R-2021-234). The authors would like to extend their sincere thanks to Dr. Sagarika Chandra for her kind help in editing images/figures incorporated in this manuscript.

References

Agarwal, S.K., Singh, S.S., Verma, S., Kumar, S., 2000. Antifungal Activity of Anthraquinone Derivatives from Rheum Emodi. J Ethnopharmacol. 72 (1-2), 43–46.

Barnham, K.J., Masters, C.L., Bush, A.I., 2004. Neurodegenerative Diseases and Oxidative Stress. Nat Rev Drug Discov. 3 (3), 205–214.

Bederson, J.B., Pitts, L.H., Germano, S.M., Nishimura, M.C., Davis, R.L., Bartkowski, H. M., 1986. Evaluation of 2,3,5-Triphenyltetrazolium Chloride as a Stain for Detection and Quantification of Experimental Cerebral Infarction in Rats. J Stroke. 17 (6), 1304–1308.

Claibome, A., 1985. Handbook of Methods for Oxygen Free Radical Research. CBC Press: Boca Raton FL 1985, 145–146.

Cristina, P.M., Cherubini, A., Stahl, W., Senin, U., Sies, H., Mecocci, P., 2002. Plasma Carotenoid and Malondialdehyde Levels in Ischemic Stroke Patients: Relationship to Early Outcome. Free Radic Res. 36, 265–268.

Dong-Ju, P., Kang, J.B., Shah, F.A., Jin, Y.B., Koh, P.O., 2020. Quercetin Attenuates Decrease of Thioredoxin Expression Following Focal Cerebral Ischemia and Glutamate-Induced Neuronal Cell Damage. Neurosci. 428, 38–49.

Emine, S., Solaroglu, I., Ozdemir, Y.G., 2018. Cell Death Mechanisms in Stroke and Novel Molecular and Cellular Treatment Options. Curr Neuropharmacol. 16, 1396–1415.

Era, T., Probert, L., 2008. Ischemic Neuronal Damage. Curr Pharm Des. 14, 3565–3573.

Farbiszewski, R., Bielawska, A., Szymanska, M., Skrzydlewska, E., 1996. Spermine Partially Normalizes in Vivo Antioxidant Defense Potential in Certain Brain Regions in Transiently Hypoperfused Rat Brain. Neurochem Res. 21 (12), 1497–1503.

Fengge, S., Ge, C., Yuan, P., 2020. Aloe-Emodin Induces Autophagy and Apoptotic Cell Death in Non-Small Cell Lung Cancer Cells via Akt/MTOR and MAPK Signaling. Eur J Pharmacol. 173550.

George, E.L., 1959. Tissue Sulfhydryl Groups. Arch Biochem Biophys. 82, 70–77.

Ginsberg, M.D., Belayev, L., ZhÅ, W., Huh, P.W., Busto, R., 1999. The Acute Ischemic Penumbra: Topography, Life Span, and Therapeutic Response. J Stroke Res Treat. 73, 45–50.

Guo, C., Wang, S., Duan, J., Jia, N.a., Zhu, Y., Ding, Y.i., Guan, Y., Wei, G., Yin, Y., Xi, M., Wen, A., 2017. Protocatechualdehyde Protects Against Cerebral Ischemia-Reperfusion-Induced Oxidative Injury Via Protein Kinase Cε/Nrf2/HO-1 Pathway. Mol Neurobiol. 54 (2), 833–845.

Hait, A.P., Ca, D., Gu, Z., Liu, G., Guo, Y., Lu, C., 2013. Bone Morphogenetic Protein-7 Ameliorates Cerebral Ischemia and Reperfusion Injury via Inhibiting Oxidative Stress and Neuronal Apoptosis. Int J Mol Sci. 14, 3441–3453.

Hitoshi, K., Ito, Y., Kitabayashi, C., Tanaka, A., Nishioka, R., Yamazato, M., Ishizawa, K., Nagai, T., Hirayama, M., Takahashi, K., Yamamoto, T., Araki, N., 2020. Effects of Edaravone on Nitric Oxide, Hydroxyl Radicals and Neuronal NitricOxide Synthase During Cerebral Ischemia and Reperfusion in Mice. J Stroke Cerebrovasc Dis. 29, 104531.

Hwang, W., Chung, J., Ho, C., Wu, L., Chang, S., 1998. Aloe-Emodin Effects on Arylamine N -Acetyltransferase Activity in the Bacterium Helicobacter Pylori. Planta Med. 64, 176–178.

Inan, O., Ozyurt, H., 2012. Reactive Oxygen Species and Ischemic Cerebrovascular Disease. Neurochem Int. 60, 208–212.
Jingxian, W., Li, Q., Wang, X., Yu, S., Li, L., Wu, X., Chen, Y., ZhÅ, J., ZhÅ, Y., 2013. Neuroprotection by Curcumin in Ischemic Brain Injury Involves the Akt/Nrf2 Pathway. Plos One. 8.
Kang, J.-B., Park, D.-J., Shah, M.-A., Koh, P.-O., 2021. Retinoic Acid Exerts Neuroprotective Effects against Focal Cerebral Ischemia by Preventing Apoptotic Cell Death. Neurosci Lett. 757, 135979. https://doi.org/10.1016/j.neulet.2021.135979.
Kumar, S., Yadav, M., Yadav, A., Rohilla, P., Yadav, J.P., 2017. Antiplasmodial Potential and Quantification of Aloin and Aloe-Emodin in Aloe Vera Collected from Different Climatic Regions of India. BMC Complem Alternm. 17, 369.
Lian, L.-H., Park, E.-J., Piao, H.-S., Zhao, Y.-Z., Sohn, D.H., 2005. H.Aloe Emodin-Induced Apoptosis in t-HSC/Cl-6 Cells Involves a Mitochondria-Mediated Pathway. Basic Clin Pharmacol Toxicol. 96 (6), 495–502.
Li, L., Xie, J., Wang, Y., Wang, S., Wu, S., Wang, Q., Ding, H., 2014. Protective Effects of Aloe-Emodin on Scopolamine-Induced Memory Impairment in Mice and H_2O_2-Induced Cytotoxicity in PC12 Cells. Bioorg Med Chem Lett. 24, 5385–5389.
Lin, L., Wang, X., 2016. Ischemia-Reperfusion Injury in the Brain: Mechanisms and Potential Therapeutic Strategies. Biochem Pharmacol. 5, 213.
Marc, S.J., Kent, T.A., Chen, M., Tarasov, K.V., Gerzanich, O., 2007. Brain Oedema in Focal Ischaemia: Molecular Pathophysiology and Theoretical Implications. Lancet Neurol. 6, 258–268.
Mavdzhuda, Z., Prosvirnina, M., Daineko, A., Simanenkova, A., Petrishchev, N., Sonin, D., Galagudza, M., Shamtsyan, M., Juneja, L.R., Vlasov, T., 2013. L-Theanine Administration Results in Neuroprotection and Prevents Glutamate Receptor Agonist-Mediated Injury in the Rat Model of Cerebral Ischemia-Reperfusion. Phytother Res. 27, 1282–1287.
Oleg, T., Olson, A.J., 2010. AutoDock Vina: Improving the Speed and Accuracy of Docking with a New Scoring Function, Efficient Optimization, and Multithreading. J Comput Chem. 31, 455–461.
PÅlo, V., Scarpa, M., Rotilio, G., Rigo, A., 1988. A Kinetic Study of the Reactions between H2O2 and Cu,Zn Superoxide Dismutase; Evidence for an Electrostatic Control of the Reaction Rate. Biochim Biophys Acta, Protein Struct Mol Enzymol. 952, 77–82.
Peter, C.J., Juliet, M., 2005. Taylor. Reactive Oxygen Species and the Modulation of Stroke. Free Radic Biol Med. 38, 1433–1444.
Sharanya, C.S., Arun, K.G., Sabu, A., Haridas, M., 2020. Aloe Emodin Shows High Affinity to Active Site and Low Affinity to Two Other Sites to Result Consummately Reduced Inhibition of Lipoxygenase. Prostag Oth Lipid M. 150, 106453. https://doi.org/10.1016/j.prostaglandins.2020.106453.
Song, W., Yan, W.W., He, M., Wei, D., Long, Z.J., TÅ, Y.M., 2020. Aloe Emodin Inhibits Telomerase Activity in Breast Cancer Cells: Transcriptional and Enzymological Mechanism. Pharm Rep. 72, 1383–1396.
Stefan, M., Gudrun, M., 1974. Involvement of the Superoxide Anion Radical in the Autoxidation of Pyrogallol and a Convenient Assay for Superoxide Dismutase. Eur J Biochem. 47, 469–474.
Tabassum, R., Vaibhav, K., Shrivastava, P., Khan, A., Ejaz Ahmed, M.d., Javed, H., Islam, F., Ahmad, S., Saeed Siddiqui, M., Safhi, M.M., Islam, F., 2013. Centella Asiatica Attenuates the Neurobehavioral, Neurochemical and Histological Changes in Transient Focal Middle Cerebral Artery Occlusion Rats. Neurol Sci. 34 (6), 925–933.
Tiansong, Y., Feng, C., Wang, D., Qu, Y., Yang, Y., Wang, Y., Sun, Z., 2020. Neuroprotective and Anti-Inflammatory Effect of Tangeretin Against Cerebral Ischemia-Reperfusion Injury in Rats. Inflammation. 43, 2332–2343.
Turley, K.R., Toledo-Pereyra, L.H., Kothari, R.U., 2005. Molecular Mechanisms in the Pathogenesis and Treatment of Acute Ischemic Stroke. J Invet Surg. 18 (4), 207–218.
Vadivel, K., Sitty, M.B., Periyannan, M., 2018. Design Synthesis in Silico in Vitro and in Vivo Evaluation of Novel L-Cysteine Derivatives as Multi-Target-Directed Ligands for the Treatment of Neurodegenerative Diseases. Beni-Suef Univ J Basic Appl Sci. 7, 452–460.
Wen, L.C., Wu, C.F., HsiÅ, N.W., Chang, C.Y., Li, S.W., Wan, L., Lin, Y.J., Lin, W.Y., 2008. Aloe-Emodin Is an Interferon-Inducing Agent with Antiviral Activity against Japanese Encephalitis Virus and Enterovirus 71. Int J Antimicrob Agents. 32, 355–359.
Wen-yi, Q., Luo, Y., Chen, L., TA, T., Li, Y., Cai, Y.L., Li, Y.H., 2013. Electroacupuncture Could Regulate the NF-KB Signaling Pathway to Ameliorate the Inflammatory Injury in Focal Cerebral Ischemia/Reperfusion Model Rats. Evid-Based Complement Altern Med. 924541, 1–15.
Wei, Z., Yuan, Y., Feng, B., Sun, Y., Jiang, H., ZhÅ, W., Zheng, Y., ZhÅ, L., Chen, T., Hang, P., Chen, Y., Dr, Z., 2021. Aloe-Emodin Relieves Zidovudine-Induced Injury in Neonatal Rat Ventricular Myocytes by Regulating the P90rsk/p-Bad/Bcl-2 Signaling Pathway. Environ Toxicol Pharmacol. 81.
Wei, T., Chen, C., Lei, X., ZhÅ, J., Liang, J., 2018. CASTp 3.0: Computed Atlas of Surface Topography of Proteins. Nucleic Acids Res. 46, 363–367.
Yasuhisa, K., 1978. Generation of Superoxide Radical during Autoxidation of Hydroxylamine and an Assay for Superoxide Dismutase. Arch Biochem Biophys. 186, 189–195.
Yu, Y., Liu, H., Yang, D., He, F., Yuan, Y., Guo, J., Hu, J., Yu, J., Yan, X., Wang, S., Du, Z., 2019. Aloe-Emodin Attenuates Myocardial Infarction and Apoptosis via up-Regulating MiR-133 Expression. Pharmacol Res. 146, 104315.
Vesna, S., Korenic, A., Radenovic, L., 2011. Spatial and Temporal Patterns of Oxidative Stress in the Brain of Gerbils Submitted to Different Duration of Global Cerebral Ischemia. Int J Dev Neurosci. 29, 645–654.
Xiong, Z., Pignataro, G., Li, M., Chang, S., Simon, R., 2008. Acid-Sensing Ion Channels (ASICs) as Pharmacological Targets for Neurodegenerative Diseases. Curr Opin Pharmacol. 8, 25–32.